J Mater Sci (2011) 46:1830–1838
DOI 10.1007/s10853-010-5008-0

Dominancy of antiferromagnetism in $Zn_{1-x}Co_xO$ diluted magnetic semiconductors

Musa Mutlu Can · Tezer Fırat · Şadan Özcan

Received: 22 July 2010 / Accepted: 14 October 2010 / Published online: 27 October 2010

Abstract The outline of magnetic interactions in DMSs was determined using $Zn_{1-x}Co_xO$ particles, where "x" was changed as 0.01, 0.05, 0.10, 0.15, and 0.20. The syntheses were accomplished though mechanical milling and thermal treatment, known as solid state reaction. The formation of each synthesis was monitored by differential thermal and thermo gravimetric methods (DT-TGA). Substitution of Co^{2+} ions with Zn^{2+} host atoms in a ZnO lattice was analyzed using X-ray diffraction (XRD) patterns, Fourier transform infrared (FT-IR) spectroscopy, energy dispersive X-ray spectrometry (EDS) data, transmission electron microscopy (TEM) figures, scanning area electron diffraction (SAED) patterns, and X-ray photo spectroscopy (XPS) spectrum. The measured Co contents in ZnO lattice were found to be $\sim$0.7% less than the expected result. In addition to $Zn_{1-x}Co_xO$ particles, tungsten (W) contaminations were noticed in the variations of $1.5 \pm 0.2\%$, as originating from the abrasion between the miller and balls. The progressive replacement of Co^{2+} with Zn^{2+} host ions in ZnO lattice from 1% to 20% decreased the band edge from 3.03 ± 0.01 eV to 2.95 ± 0.01 eV, respectively. Co doping has also changed the magnetic nature of the ZnO. Although having both interactions (ferromagnetic and antiferromagnetic), dominance of ferromagnetic behavior was only observed for $Zn_{0.99}Co_{0.01}O$ with the coercivity of $\sim 154 \pm 50$ Oe and positive Curie–Weiss temperature as 79 ± 1 K. However, the calculated $\frac{2J_{ex}}{k_B}$ values have proved that the higher Co^{2+} concentrations in ZnO lattice have increased the efficiency of antiferromagnetic interactions. Surprisingly, there was no rapid change at $\frac{2J_{ex}}{k_B}$ values as mentioned in previous works.

M. M. Can (✉) · T. Fırat · Ş. Özcan
Department of Physics Engineering, University of Hacettepe, 06800 Beytepe, Ankara, Turkey
e-mail: musamutlucan@gmail.com

Introduction

A small amount of transition metal doped semiconductors, known as diluted magnetic semiconductors (DMSs) [1], have been used extensively because they are good candidates for the room temperature spintronic applications [1–4]. The wisdoms about ferromagnetism, based on polarized spins, are constructed on three suppositions. The first theory depended on the calculations of p-type doped DMSs, which pointed out p–d hybridization between the located shallow acceptors and local spins [5]. The second theory pointed out shallow donors due to s–d interactions for n-type doped DMSs [6]. The third theory, also known as d^0 ferromagnetism, originated from hybridization between the impurity bands of defects and $3d$ bands [7]. The calculations also proved that at high Curie temperature (over room temperature) ferromagnetism can be formed under p–d coupling [5]; such as oxide diluted magnetic semiconductor (O-DMS). The result of a strong exchange coupling between oxygen $2p$ and d shells of transition metals makes O-DMSs good candidates for high T_c DMSs [6, 8].

One of the widely investigated O-DMSs is Co doped ZnO. Transition metal doped ZnO structures have been essential over two decades because of the uncertainties on magnetism of these structures. The recent theoretical works pointed out p–d hybridization as the reason of the stability of ferromagnetism in p-type ZnO [5, 9] and n-type doping as the stability of antiferromagnetic behavior [9]. Recent

experiments also pointed out that either p-type doping or vacancies are the reason of the ferromagnetism [10]. Either ferromagnetic ordering or antiferromagnetic ordering is related to the unexpected compounds, which are the metallic clusters [11–14] and the oxide states of transition metals [11], respectively.

This study is the continuation of the previous work, in which 1% Co doped ZnO alloys were examined [15]. The previous work showed the inefficaciousness of the contamination W atoms on magnetic behavior and the results of both antiferromagnetic and ferromagnetic interactions [15] in the 1% Co doped ZnO. $Zn_{1-x}Co_xO$ ($x = 0.01, 0.05, 0.10, 0.15, 0.20$) structures that were synthesized with same the procedure, which employed solid state reaction process by mechanical milling and thermal treatment. This study reinforces the supposition on the dependency of antiferromagnetism to Co amount inside the ZnO lattice.

Experiments

Co doped ZnO alloys were synthesized with the same procedure as explained in detail of our previous work [15]. The basis of this process depends on precise milling and thermal treatment. The possible solid state reactions during the thermal treatment were monitored with differential thermal and thermo gravimetric analysis (DT-TGA) employing TG/DTA6300 model spectrometer under oxygen flow at 40 mL/min with α-Al_2O_3 reference container. The heating rate is 15 °C/min in the temperature range of 30–900 °C. According to the findings of these thermal analyses, the milled samples were soaked for 3 h at 900 °C.

Structural studies were accomplished using X-ray diffraction (XRD) and Fourier transforms infrared (FT-IR) measurements. Rigaku model diffractometer with Cu K_α radiation was used to obtain the XRD patterns. The scanning rate was 0.02°/min in the range of 10–90°. FT-IR measurements were done by MATTSON 1000 spectrometer after pressing at 10 tons in KBr in 400–4000 cm^{-1} range with step of 2 cm^{-1}.The particles size and electron diffraction were examined using transmission electron microscopy (TEM) and scanning area electron diffraction (SAED) pictures, respectively, which were taken by JEOL 2100F model TEM with 200 kV field emission gun. Co atoms in the ZnO lattice were detected by X-ray photoelectron spectrometer (XPS). XPS measurements were done under 234 W power with monochromate AlK_α radiation between 0 and 1200 eV energy range with 0.10 eV steps.

The elemental analyses of the samples were done by energy dispersive X-ray spectrometry (EDS), Bruker-Axs XFlash 3001 SDD/EDS spectrometer.

The optical properties were studied by UV–Visible (UV–Vis) absorption spectrometer. The model of used UV–vis absorption spectrometer was Shimadzu UV-3600/UV–VIS-NIR spectrophotometer equipped with Praying Mantis in wavelength range of 200–1500 nm.

Lastly, after collecting information about the locations of Co atoms in the lattice, the effects of Co atoms on magnetic behavior were investigated with vibrating sample magnetometer (Quantum Design-VSM) of physical properties measurement system (Quantum Design-PPMS). Magnetization versus magnetic field curves at 300 K and 10 K were obtained between ±20 kOe. DC magnetic susceptibility (χ) versus temperature (T) measurements was done in temperature range of 10–300 K.

Results and discussion

The thermal treatments of milled precursor powders were done to obtain the optimum values of DT-TGA measurements. A typical DT-TGA spectrum was given in Fig. 1, which was obtained for $Zn_{0.9}Co_{0.1}O$. As seen in figure, heating around 100–130 °C decreased the mass of samples, observed from thermo gravimetric (TG) investigations, due to the losing water molecules. In contrast, the increase at mass was observed between 300 and 700 °C due to taking in oxygen atoms from the environment. Differential thermo gravimetric (DT) analysis was also demonstrated in the same figure, Fig. 1. Both physical conditions happened as endothermic reactions since the maxima of the temperatures are 125.0 ± 0.5 °C and 418.0 ± 0.3 °C, respectively. No change in the mass or any thermal activity was observed over 800 °C. Then, the samples were heated from room temperature to 900 °C and were soaked at this temperature for 4 h.

X-ray diffraction (XRD) patterns of sintered samples are illustrated in log scale in Fig. 2. All patterns are in accord

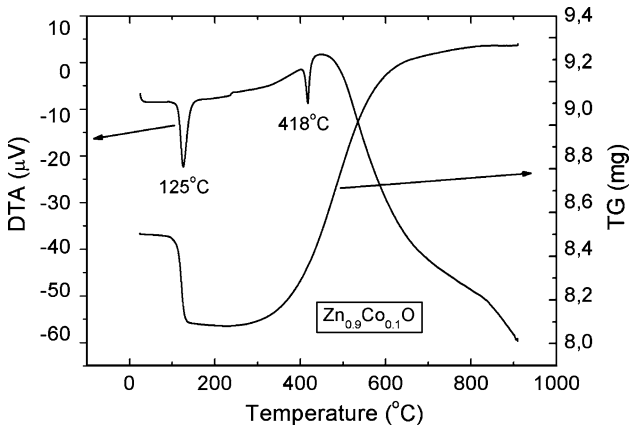

Fig. 1 DT-TGA results of $Zn_{0.9}Co_{0.1}O$ sample after milling process

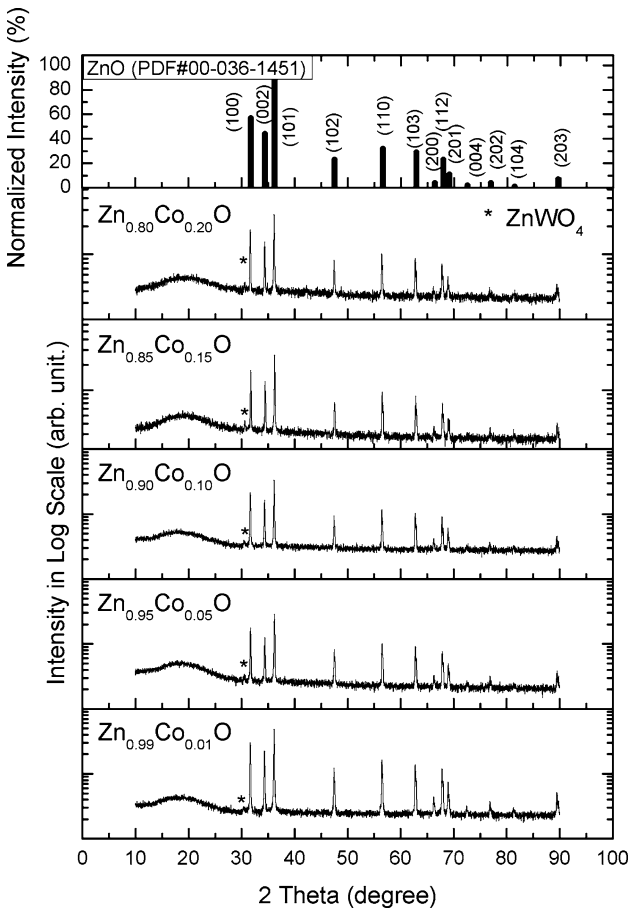

Fig. 2 X-ray diffraction patterns of synthesized $Zn_{1-x}Co_xO$ ($x = 0.01$, 0.05, 0.10, 0.15, and 0.20) diluted magnetic semiconductors

with Zincite (ZnO) which has the ICDD card PDF#00-036-1451. In addition to ZnO, $ZnWO_4$ (PDF#00-015-0774) is also observed as the secondary phase. The WC vial and balls (consist of 94% W and 6% Co) were the sources of W contaminations. Nonetheless, the peaks from Co clusters or oxidized states of Co were not detected. The disagreement on the solubility limit of Co atoms continues to understand in literature. The argument is on the possibility of solving over the 10% Co atoms in ZnO; however, all researches have accepted the possibility up to the used technique in synthesis [9, 16]. Alternatively, in the 15 and 20% doped ZnO samples, it is possible for the secondary phases such as Co_3O_4. Due to the detection limit of XRD, it is difficult to exclude the presence of those particles.

Rietveld analyses of the samples were determined by JADE8 program using the two theta values, which were indexed with (100), (002), (101), (102), (110), (103) and (112). The structure is fitted to the hexagonal ZnO (the ICDD card PDF#00-036-145), which has P63mc space group with lattice parameters $a = 3.24982$ Å and $c = 5.2066$ Å. The calculated lattice constants are shown in Table 1. A gradual increase at the "a" parameter has been observed, dependent on the doping Co atoms in ZnO lattice. In contrast, "c" parameters are almost same to the each other and the values are very close to the literature. According to these results, it can be figured out that the Co^{2+} ions have been substituted by the host Zn^{2+} ions in tetrahedral coordinate because of the close ionic radius of Zn^{2+} (0.60 Å) ions to Co^{2+} ions (0.58 Å) at these coordinates [9, 17, 18]. The radius of Co^{2+} ions at octahedral site is between the 0.65 Å (low spin state) and 0.745 Å (high spin state) [9, 18]. According to these values, a large difference at the lattice parameters has been expected if Co^{2+} ions are located in octahedral site. Moreover, it can also be figured out that there are no any Co^{3+} ions, where ionic radius is lower than Co^{2+} [17], in the lattice due to not having a prominent change in lattice parameters.

Energy dispersive X-ray spectrometry (EDS) measurements were also taken due to the deficiency of XRD patterns for the detection of Co atoms. EDS picture has been shown in Fig. 3 only for the sample of $Zn_{0.80}Co_{0.20}O$. The normalized atomic values are shown in Table 2. The given data are the average values of four different regions. It is observed that the atomic percentage of Zn and Co atoms are close to the values what they were expected. In addition, the percent of W contamination atoms have been found in the range of $1.5 \pm 0.3\%$.

TEM and SAED figures were used to examine according to the confirmation of Co metal and Co clusters exist in the host as shown in Fig. 4. The pictures of $Zn_{0.80}Co_{0.20}O$ particles were demonstrated in Fig. 4, because of not having any change in synthesize parameters for all samples. If there are no any clues about the formation of other components, it should be the same for all others. The smallest particles were observed in size range from 100 to 500 nm, which is very high value to be nanosize. Because of having huge particle size, the electron diffraction patterns of the samples were not observed as a circular shape. The SAED patterns, shown inner picture of Fig. 4, were

Table 1 Lattice parameter of synthesized $Zn_{1-x}Co_xO$ ($x = 0.00$, 0.01, 0.03, 0.05, and 0.10) diluted magnetic semiconductors, determined by 2 thetas of XRD patterns with using of subprogram of "JADE8"

Lattice parameters of $Zn_{1-x}Co_xO$	$x = 0.01$	$x = 0.05$	$x = 0.10$	$x = 0.15$	$x = 0.20$
a (Å)	3.2504 ± 0.0003	3.2520 ± 0.0003	3.2521 ± 0.0004	3.2536 ± 0.0006	3.2542 ± 0.0007
c (Å)	5.2049 ± 0.0003	5.2057 ± 0.0004	5.2047 ± 0.0005	5.2062 ± 0.0006	5.2042 ± 0.0007

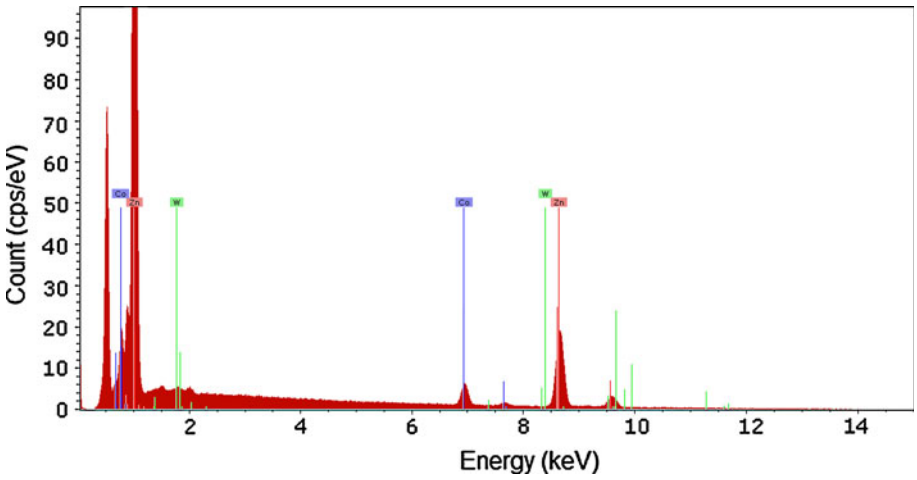

Fig. 3 EDS spectrum of $Zn_{0.80}Co_{0.20}O$ particles

Table 2 Determined atomic percent of elements of $Zn_{1-x}Co_xO$ structures by EDS measurements

	Normalized atomic percent of cobalt (%)	Normalized atomic percent of zinc (%)	Normalized atomic percent of tungsten (%)
$Zn_{0.99}Co_{0.01}O$	0.9 ± 0.1	96.9 ± 0.8	1.6 ± 0.2
$Zn_{0.95}Co_{0.05}O$	4.7 ± 0.9	93.6 ± 0.7	1.7 ± 0.1
$Zn_{0.90}Co_{0.10}O$	8.9 ± 0.7	89.5 ± 0.1	1.5 ± 0.2
$Zn_{0.85}Co_{0.15}O$	14.2 ± 0.3	84.7 ± 0.2	1.1 ± 0.1
$Zn_{0.80}Co_{0.20}O$	19.5 ± 0.2	78.7 ± 1.0	1.8 ± 0.1

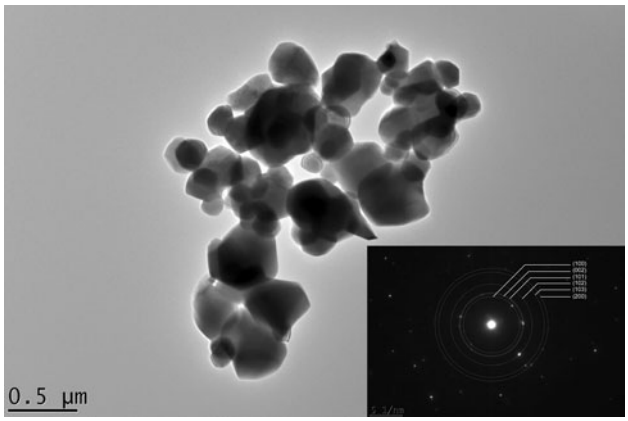

Fig. 4 TEM figure of the $Zn_{0.80}Co_{0.20}O$ particles. The inset is the SAED picture of the particles with simulated patterns of ZnO

simulated to the circles to point out the patterns. The (100), (002), (101), (102), (103) and (200) diffractions from ZnO structure were pointed on the SAED picture. The diffractions from $ZnWO_4$ were not detected, which were detected in the XRD patterns.

Fourier transform infrared (FT-IR) measurements have been utilized to understand the existence of Co in ZnO as presented in Fig. 5 and the results have been given in Table 3. The absorption bands were observed at around 449 ± 3 cm^{-1}, 484 ± 2 cm^{-1}, and 529 ± 2 cm^{-1} which belong to ZnO [19, 20]. Additionally, there was a shift at the absorption bands, depending on impurity ions that are substituted with Zn^{2+} in tetrahedral lattice [21]. These values were totally different from the absorption bands of stretching vibration between the Co–O bonds in Co_3O_4 [22, 23] as summarized in Table 3.

In order to confirm the substitution of Co^{2+} ions with the host Zn^{2+} ions in ZnO lattice, the XPS measurements were done. The spectra in Fig. 6 were arranged according to the C1*s* binding energy, 285 eV. The Co atoms in ZnO lattice were determined by the splits of Co2*p* electronic states. The valance states of Co atoms [24, 25] lead the difference at Co2*p* binding energy states, $Co2p_{3/2}$ and $Co2p_{1/2}$. The average value of energy differences of our samples is 16.1 ± 0.2 eV as shown in Fig. 6. This indicates that there is no any Co cluster in our samples due to lack of the same energy difference of Co cluster, ~15.05 eV [24, 26]. Even though the closest energy differences of Co2*p* between Co atoms in ZnO lattice and Co atoms in Co_3O_4, the shift of the $Co2p_{3/2}$ from 779.8 to 781.40 ± 0.06 is the reason of Co atoms in ZnO lattice [25, 27]. As Gauss fits is shown in Fig. 6, the energy peaks were fit to the 4 peaks. The calculated positions are the average values of $Co2p_{3/2}$, satellite of $Co2p_{3/2}$, $Co2p_{1/2}$ and satellite of $Co2p_{1/2}$, which are 781.40 ± 0.06 eV, 786.3 ± 0.2 eV, 797.49 ± 0.08 eV, and 802.3 ± 0.1 eV, respectively. These values are compatible with the literature at reference [28] to be Co^{2+} ions in ZnO lattice. The energy differences and located binding energy positions also indicate +2 electronic valance state of Co and the shift at the peak position of $Co2p_{3/2}$ states to the higher energies depending on the Co atoms in ZnO lattice [26, 27, 29].

The optical analyses, done by the UV–Vis data, give information about the band edge change, the electronic states, and electronic transitions. The electronic states of Co^{2+} ions were found as $3d^7$ electronic ordering with

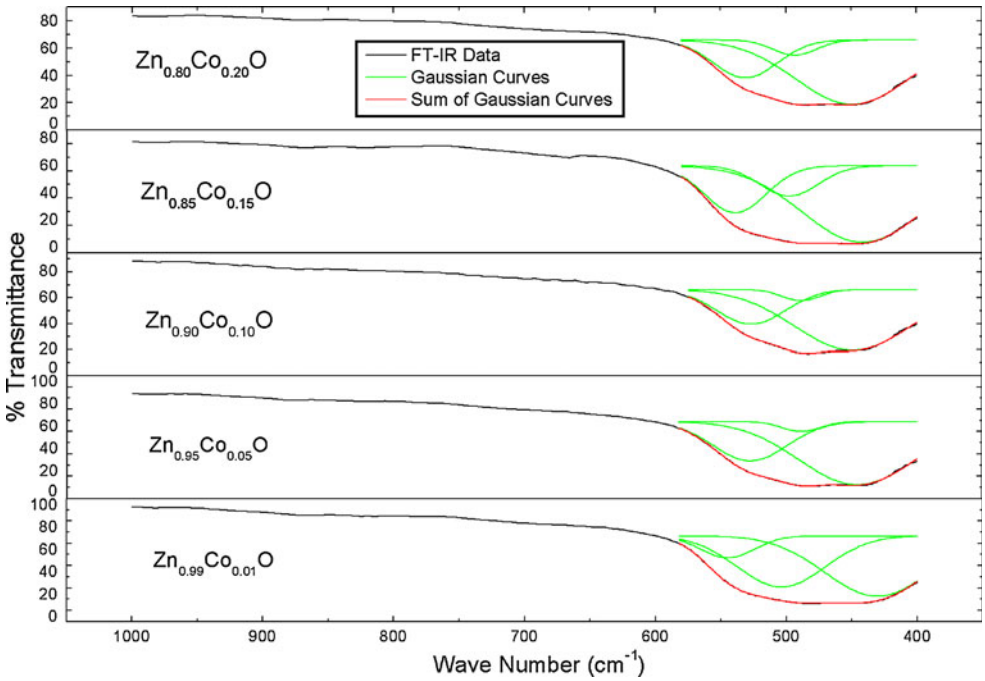

Fig. 5 Fourier transform infrared patterns of synthesized $Zn_{1-x}Co_xO$ ($x = 0.01$, 0.05, 0.10, 0.15 and 0.20) diluted magnetic semiconductors

Table 3 FT-IR measurements of $Zn_{1-x}Co_xO$ structures

Sample	FT-IR wave numbers (cm^{-1}) ± 1		
$Zn_{0.99}Co_{0.01}O$	546	504	429
$Zn_{0.95}Co_{0.05}O$	527	489	447
$Zn_{0.90}Co_{0.10}O$	527	489	448
$Zn_{0.85}Co_{0.15}O$	539	498	443
$Zn_{0.80}Co_{0.20}O$	530	494	449
ZnO	529 [19, 20]	494 [19, 20]	443 [19, 20]
Co_3O_4	~670 (Due to Co^{2+} ions in tetrahedral state) [22, 23]	580 (Due to Co^{+3} ions in octahedral state) [22, 23]	

tetrahedral symmetry at ground state of $^4A_2(F)$. Because of substitution of Co^{2+} with Zn^{2+} ions in lattice, three types of permitted transitions between intra ionic d–d^* were observed. These transitions are demonstrated in Fig. 7 at 1311 ± 10 nm, 1417 ± 10 nm ($\nu_2(Co^{2+}_{Td})$: $^4T_1(F) \rightarrow {}^4A_2(F)$) and 564 ± 2 nm, 613 ± 4 nm, 657 ± 5 nm ($\nu_3(Co^{2+}_{Td})$: $^4T_1(P) \rightarrow {}^4A_2(F)$) and increasing intensities by amount of Co ions can be related to be in high spin states of Co^{2+}.

The energy band gap of ZnO is 3.35 eV and the absorption edge of this is around 370 nm for bulk state [30, 31]. Enrichment of Co atoms inside the ZnO lattice narrowed the band gap due to *sp-d* hybridization [32]. In the study, the band gaps were not observed as known that there exists a charge transfer process from a Co^{2+} ion to Co^{1+} ion, which is strongly reflected in an absorption spectrum near the band edge [33]. Therefore, it is rather difficult to estimate a "band gap" without using magnetic circular dichroism (MCD) spectroscopy. However, the found value about band edge is compatible to the results as shown in Fig. 7. The figure has clearly illustrated ZnO band edge change due to the shift of the decrease at the absorption curve (between the wavelength of 332 and 487 nm) to the right. The band edges were also calculated by using the climacteric points of the curves, which were calculated by taking the derivation of the interval 332 and 487 nm,. The calculated band edges are 3.03 ± 0.01 eV, 2.88 ± 0.01 eV, 2.86 ± 0.01 eV, 2.84 ± 0.01 and 2.80 ± 0.01 eV for $x = 0.01, 0.05, 0.10, 0.15$, and 0.20, respectively.

Magnetic effect of substitution Co^{2+} ions with Zn^{2+} in ZnO lattice were analyzed by magnetization versus magnetic field ($\sigma(H)$) at 10 K and 300 K temperatures, magnetization versus temperature ($\sigma(T)$) curves and inverse DC magnetic susceptibility versus temperature ($\chi^{-1}(T)$) curves in temperature range of 10–300 K as illustrated in Fig. 8. The smooth change was observed in $\sigma(T)$ curves until to around 70 K. After temperature 70 K, rapid enhancement at the magnetization was observed. The characteristic of $\sigma(T)$ curves are coherent to the Curie–Weiss law as shown in Fig. 8a.

The $\chi^{-1}(T)$ curves, shown in Fig. 8a, b, were formulized by Curie–Weiss expression [9, 16, 17], in Eq. 1, in order to determine the effect of antiferromagnetic behavior.

$$\frac{1}{\chi} = \frac{(T+\theta)}{C} \tag{1}$$

θ and C are the Curie–Weiss temperature and the Curie constant, respectively. The linear fits were done in

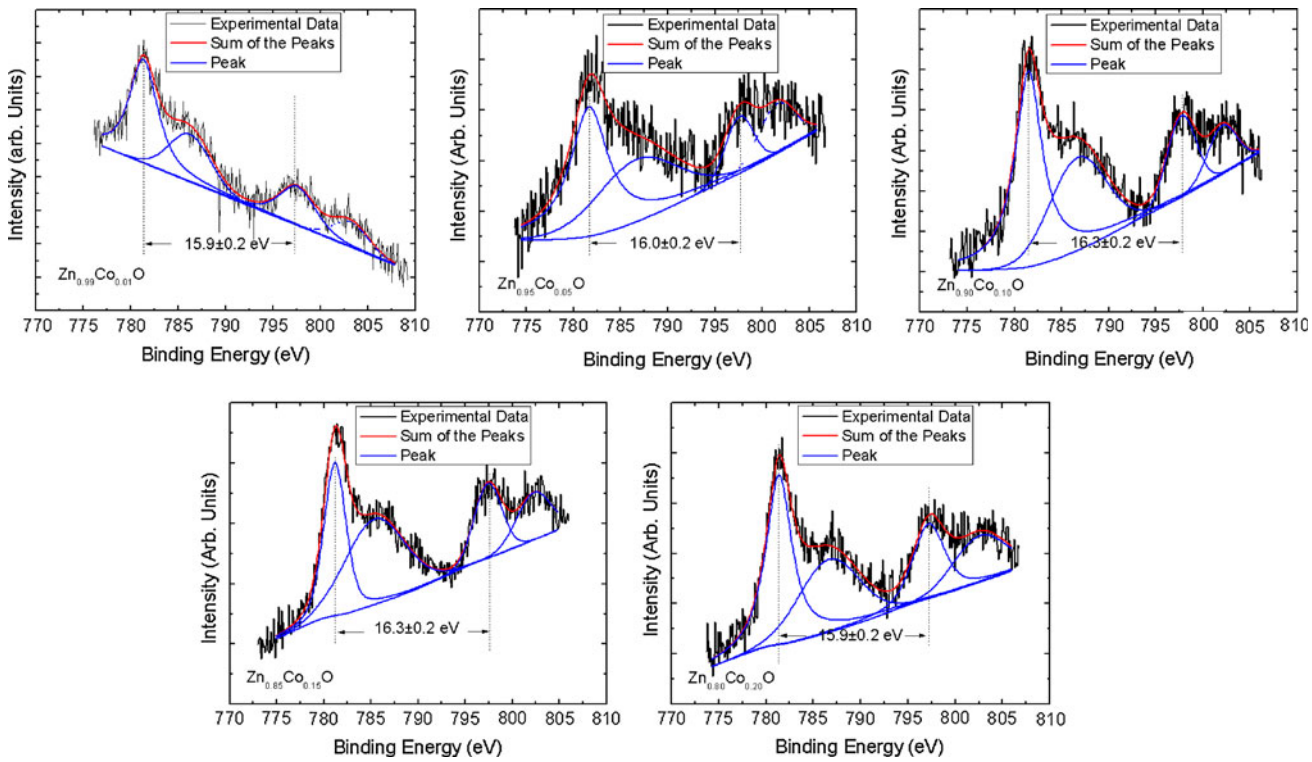

Fig. 6 X-ray photo spectroscopy spectrums of synthesized $Zn_{1-x}Co_xO$ ($x = 0.01$, 0.05, 0.10, 0.15, and 0.20) diluted magnetic semiconductors as the characteristic binding energies of Co2*p*

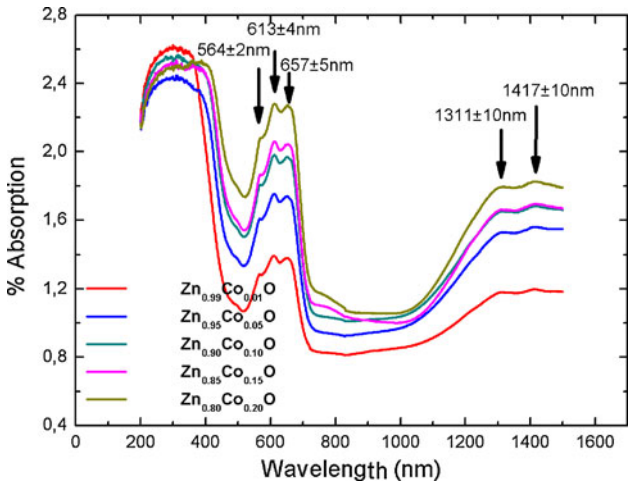

Fig. 7 UV–vis absorption spectrums of synthesized $Zn_{1-x}Co_xO$ ($x = 0.01$, 0.05, 0.10, 0.15 and 0.20) diluted magnetic semiconductors

temperature range 76–300 K except $Zn_{0.99}Co_{0.01}O$ as seen in Fig. 8a and for $Zn_{0.99}Co_{0.01}O$ in temperature range of 210–300 K, where the linearity was observed. The calculated θ, C, and effective magnetic moment (μ_{eff}) values are shown in Table 4. The decrease is observed at the "θ" values versus Co amount in ZnO lattice and having negative signs prove the dominancy of antiferromagnetic interactions, except $Zn_{0.99}Co_{0.01}O$. In addition, "μ_{eff}" values in Table 4 were calculated by using expression of (2).

$$\mu_{eff} = \sqrt{\frac{3k_B C M_W}{N}} \tag{2}$$

k_B, C, M_w, and N are Boltzmann constant (1.38×10^{-16}erg/K), Curie constant, molecular weight of $Zn_{1-x}Co_xO$ (81.3254 a.u, 81.067 a.u., 80.744 a.u.,80.421 a.u. and 80.098 a.u for amount of $x = 0.01$, 0.05, 0.10, 0.15, and 0.20, respectively) and Avogadro number (6.02×10^{23}), respectively. Co^{2+} ions have three uncoupled electrons with d^7 high spin state and the calculated spin based magnetic moment value is 3.0 μ_B [9]. In our study, the calculated "μ_{eff}" values are smaller than the value in literature. The result shows that few amount of Co ions coupled as ferromagnetically and the others coupled as paramagnetic or antiferromagnetically due to super exchange interaction. The competitions between ferromagnetic and antiferromagnetic interactions are the reason of small μ_{eff} values. The best way of determining the effectiveness of super exchange interaction is to find effective exchange interaction constant (J_{ex}) [16, 17, 34]. There are different suggestions at the usage of theoretical findings of "$\frac{2J_{ex}}{k_B}$" values. Kolesnik et al. [17] used the theoretical "g (Lande g factor)" and "J" values. Alternatively, Mandal et al. [16] and Kane et al. [34] used

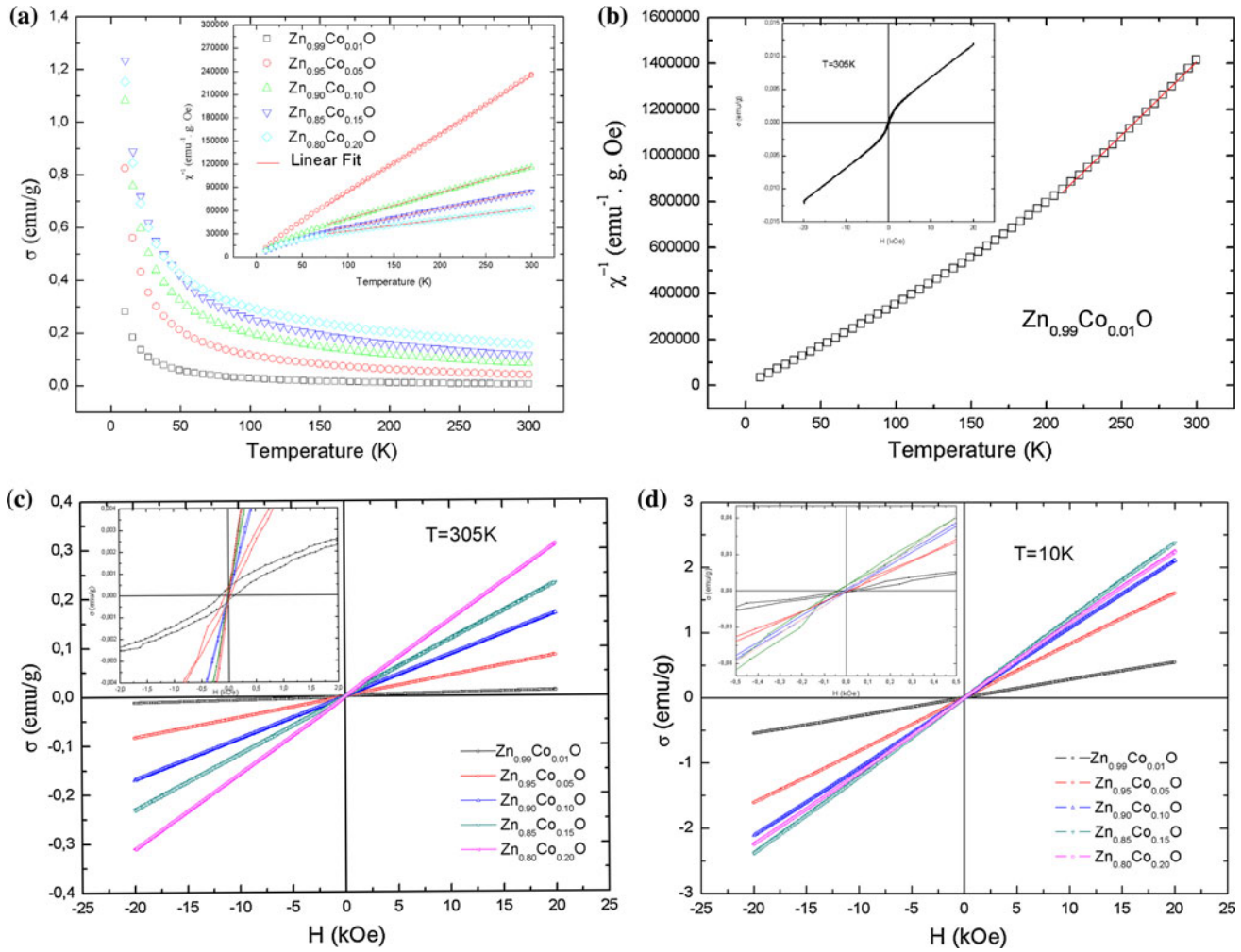

Fig. 8 **a** Magnetization versus temperature and inverse DC magnetic susceptibility versus temperature curves of $Zn_{1-x}Co_xO$ ($x = 0.01$, 0.05, 0.10, 0.15, and 0.20) in temperature range of 10–300 K, **b** inverse DC magnetic susceptibility versus temperature curves of $Zn_{0.99}Co_{0.01}O$ in temperature range of 10–300 K (the inset shows magnetization versus magnetic field curves of $Zn_{0.99}Co_{0.01}O$ at 305 K), and magnetization versus magnetic field curves at (**c**) 10 K and (**d**) 300 K (the inset shows expended view of magnetization versus magnetic field curves near the origin). *Red* lines demonstrated linear fit to Curie–Weiss law

theoretical calculated "g" values and experimentally found "J".

In this study, Eq. 3 was used to release the theoretical values and the equation of "$\frac{2J_{ex}}{k_B}$" was rearranged as Eq. 4.

$$\mu_{\text{eff}} = g\sqrt{j(j+1)}\mu_B \tag{3}$$

$$\left(\frac{2J_{ex}}{k_B}\right) = \frac{3\theta}{Z_{NN}g^2\left(\frac{\mu_{\text{eff}}}{\mu_B}\right)^2} \tag{4}$$

Z_{NN} is equal to 12, the number of nearest neighbors in hexagonal ZnO. In the Eq. 4, there is no need to consider the molar Curie–Weiss temperature like the other studies [17, 33, 34]. By rearranging the equation, it is decided to find the effective exchange interaction of the whole atoms in the lattice, not just only the transition metals in the lattice. The calculations are demonstrated in Table 4. The values with negative signs of $\left(\frac{2J_{ex}}{k_B}\right)$ also proved the antiferromagnetic interaction. After 10% Co doping, it was not observed any specific change depending on Co^{2+} amounts.

As presented in Fig. 8b, only for $Zn_{0.99}Co_{0.01}O$ particles, the ferromagnetic interactions are dominant, so hysteresis can easily be observed. The coercivity at 305 K is 154 ± 50 Oe (the written error is originating from the system measurement). The other $\sigma(M)$ curves for 305 K and 10 K are illustrated in Fig. 8c, d, respectively. The linearity of $\sigma(M)$ curves were perfect by increase of x (doped ratio of Co) which indicated magnetic ordering as paramagnetic.

These results are in agreement with the previous studies in which they increased the x values in $Zn_{1-x}Co_xO$ [9, 16, 35]. They all observed that the increase of x value enhanced the antiferromagnetic behave. The common idea

Table 4 The calculated θ, C, μ_{eff}, and $\left(\frac{J_{ex}}{k_B}\right)$ values according to the Curie–Weiss law

The ratio of doped Co atoms in $Zn_{1-x}Co_xO$	$x = 0.01$	$x = 0.05$	$x = 0.10$	$x = 0.15$	$x = 0.20$
θ (K)	79 ± 1	-12.9 ± 0.6	-50.9 ± 0.4	-69.5 ± 0.8	-126.9 ± 0.2
C (emu.K/g.Oe) $\times 10^{-4}$	1.6 ± 0.1	13.3 ± 0.3	29.9 ± 0.1	43.1 ± 0.1	66.9 ± 0.3
μ_{eff} (μ_B)	0.32 ± 0.01	0.93 ± 0.01	1.39 ± 0.02	1.67 ± 0.02	2.07 ± 0.05
$\frac{2J_{ex}}{k_B}$(K)	$\frac{192\pm1}{g^2}$	$\frac{-3.7\pm0.6}{g^2}$	$\frac{-6.6\pm0.4}{g^2}$	$\frac{-6.2\pm0.8}{g^2}$	$\frac{-7.4\pm0.2}{g^2}$

is the enhancements of antiferromagnetic interactions depending on the amount coupled Co^{2+} cations in the lattice. The limit value is 5%, enough to couple all magnetic ions with others as mentioned in the study of Risbud et al. [9]. However, it is not possible to ignore the ferromagnetic character because of propositions of all approaches [9, 16, 35–38]. Magnetic ions (Co, Mn, …etc.) couplings mean the decreased distance according to uncoupled states. They interact with each others under oxygen mediation which is known as superexchange interaction (origin of antiferromagnetism). In addition, the isolated Co cations do not interact with other magnetic ions. The theoretical approximations demonstrated ferromagnetic ordering for these isolated cations [36]. However, the over limit (more than 5%) doping magnetic ions make all ions couple to each other, and finally the only interactions develop into the antiferromagnetic interaction.

Conclusions

The results are important to complete the previous study. The study presented that mechanical milling and thermal treatment are also successful to synthesize $Zn_{1-x}Co_xO$ ($x = 0.01$, 0.05, 0.10, 0.15 and 0.20) diluted magnetic semiconductors. The structural analyses showed that the settled Co^{2+} ions to the tetrahedral lattice with high spin state. No any oxide compounds of Co or Co cluster were found in the structure. However, it was figured out that secondary phase of $ZnWO_4$, formed during the solid state reaction. The contamination of W was originated from the mechanical miller and the balls.

The $\chi^{-1}(T)$ curves proved that the enhancement of the amount of substituted Co^{2+} ions in lattice makes the antiferromagnetic interaction increase. The ferromagnetic behavior was only observed for $Zn_{0.99}Co_{0.01}O$ particles as figured out from positive Curie–Weiss temperature; however, it is not possible to ignore the antiferromagnetic effect because of lower μ_{eff} values than expected. The ferromagnetic character of $Zn_{0.99}Co_{0.01}O$ is also determined by the measurements of $\sigma(H)$ at 305 K with the coercivity of $\sim 154 \pm 50$ Oe. This hysteresis disappeared at 10 K which can be related to the domination of antiferromagnetism at low temperature. The hysteresis was not observed for the other $\sigma(H)$ curves of $Zn_{1-x}Co_xO$ structures neither 10 K nor 305 K.

Acknowledgements We thank Prof. Dr. B. Karan and Dr. H. Erdoğan for the UV–vis. and FT-IR measurements, the members of Department of Chemistry, Hacettepe University, and Dr. E. Çubukçu and Prof. Dr. E. Aydar for EDS measurements, the members of Department of Geology Engineering, Hacettepe University. This project has been supported by Hacettepe University with project number of HÜ BAB 0901-602006.

References

1. Dietl T (2007) J Phys Condens Matter 19:165204
2. Akinaga H, Ohno H (2002) IEEE Trans Nanotechnol 1(1):19
3. Munekata H, Ohno H, Von Molnar S, Segmuller A, Chang LL, Esaki L (1989) Phys Rev Lett 63:1849
4. Ohno H, Shen A, Matsukura F, Oiwa A, Endo A, Iye Y (1996) Appl Phys Lett 69:363
5. Dietl T, Ohno H, Matsukura F, Cibert J, Ferrand D (2000) Science 287:1019
6. Coey JMD, Venkatesan M, Fitzgerald CB (2005) Nat Mater 4:173
7. Coey JMD (2005) Sol Stat Sci 7:660
8. Fukumura T, Yamada Y, Toyosaki H, Hasegawa T, Koinuma H, Kawasaki M (2004) Appl Surf Sci 223:62
9. Risbud AS, Spaldin NA, Chen ZQ, Stemmer S, Seshadri R (2003) Phys Rev B 68:205202
10. Kapilashrami M, Xu J, Ström V, Rao KV, Belova L (2009) Appl Phys Lett 95:033104
11. Calderon MJ, Das Sarma S, arxiv: Cond-Mat/0603182v2 [cond-mat.mtrl-sci] 11 Dec 2006
12. Janisch R, Gopal P, Spaldin N (2005) J Phys Condens Matter 17:R657
13. Park JH, Kim MG, Jang HM, Ryu S, Kim YM (2004) Appl Phys Lett 84(8):1338
14. Norton DP, Overberg ME, Pearton SJ, Pruessner K, Budai JD, Boatner LA, Chisholm MF, Lee JS, Khim ZG, Park YD, Wilson RG (2003) Appl Phys Lett 83(26):5488
15. Can MM, Firat T, Özcan S (2010) IEEE Trans Magn 46(6):1809
16. Mandal SK, Das AK, Nath TK, Karmakar D, Satpati B (2006) J Appl Phys 100:104315
17. Kolesnik S, Dabrowski B, Mais J (2004) J Appl Phys 95(5):2582
18. Jayakumar OD, Gopalakrishnan IK, Kulshreshtha SK (2005) J Mater Chem 15:3514
19. Kleinwechter H, Janzen C, Knipping J, Wiggers H, Roth P (2002) J Mater Sci 37:4349. doi:10.1023/A:1020656620050
20. Xiong G, Pal U, Serrano JG (2007) J Appl Phys 101:024317

21. Luo J, Xing X, Yu R, Xing Q, Zhang D, Chen X (2005) J Alloy Compd 402:263
22. Pejova B, Isahi A, Najdoski M, Grozdanov I (2001) Mater Res Bull 36:161
23. Lin H-K, Chiu H-C, Tsai H-C, Chien S-H, Wang C-B (2003) Catal Lett 88(3–4):169
24. Naeem M, Hasanain SK, Kobayashi M, Ishida Y, Fujimori A, Buzby S, Shah SI (2006) Nanotechnology 17:2675
25. Hays J, Reddy KM, Graces NY, Engelhard MH, Shutthanandan V, Luo M, Xu C, Giles NC, Wang C, Thevuthasan S, Punnoose A (2007) J Phys Condens Matter 19:266203
26. Lee H-J, Jeong S-Y, Cho CR, Park CH (2002) Appl Phys Lett 81(21):4020
27. Petitto SC, Langel MA (2004) J Vac Sci Technol A 22(4):1690
28. Wei L, Li Z, Zhang WF (2009) Appl Surf Sci 255:4992
29. Manivannan A, Seehra MS, Majumder SB, Katiyar RS (2003) Appl Phys Lett 83(1):111
30. Peng YZ, Liew T, Song WD, An CW, Teo KL, Chong TC (2005) J Supercond Nov Magn 18(1):97
31. Daniel MF, Desbat B, Lassegues JC, Gerand B, Figlarz M (1987) J Solid State Chem 67:235
32. Naeem M, Hasanain SK, Mumtaz A (2008) J Phys Condens Mater 20:025210
33. Xiao Z, Matsui H, Hasuike N, Harima H, Tabata H (2008) J Appl Phys 103:043504
34. Kane MH, Shalini K, Summers CJ, Varatharajan R, Nause J, Vestal CR, Zhang ZJ, Fersguson IT (2005) J Appl Phys 97:023906
35. Lawes G, Risbud AS, Ramirez AP, Seshadri Ram (2005) Phys Rev B 71:045201
36. Wolff PA, Bhatt RN, Durst AC (1996) J Appl Phys 79(8):5196
37. Martínez B, Sandiumenge F, Balcells Ll, Arbiol J, Sibieude F, Monty C (2005) Phys Rev B 72:165202
38. Bouloudenine M, Viart N, Colis S, Kortus J, Dinia A (2005) Appl Phys Lett 87:052501